Laser pulse duration effects in Xe2+ ions induced by multiphoton absorption at 0.53 μm

A. L'Huillier, L.A. Lompre, G. Mainfray, C. Manus

J. Physique **44** (1983) 1247-1255 NOVEMBRE **1983**, PAGE 1247

Classification
Physics Abstracts
32.80K

Laser pulse duration effects in Xe^{2+} ions induced by multiphoton absorption at 0.53 μm

A. L'Huillier, L. A. Lompré, G. Mainfray and C. Manus

Centre d'Etudes Nucléaires de Saclay, Service de Physique des Atomes et des Surfaces, 91191 Gif-sur-Yvette Cedex, France

(*Reçu le 6 avril 1983, révisé le 7 juin, accepté le 6 juillet 1983*)

Résumé. — L'ionisation multiphotonique d'atomes de xénon à 0,53 μm produit des ions Xe^{2+}. Deux processus différents donnent naissance à ces ions Xe^{2+}. A faible éclairement laser, ils sont formés par absorption de 15 photons lors d'une interaction laser-atomes de xénon. Puis en augmentant l'éclairement laser, les ions Xe^{2+} résultent d'une interaction laser-ions Xe^{+} par absorption de 10 photons à partir de l'ion Xe^{+} dans son état fondamental. Le premier processus est extrêmement sensible à la durée de l'impulsion laser qu'on a fait varier entre 5 et 200 ps. Ainsi le nombre d'ions Xe^{2+} augmente d'un facteur 30 en diminuant la durée de l'impulsion laser de 30 à 5 ps pour un éclairement laser approximativement égal à 10^{12} W.cm^{-2}. Nous avons développé un modèle théorique basé sur les équations d'évolution des populations des atomes neutres, des ions Xe^{+} et des ions Xe^{2+}. Ce modèle reproduit très bien les résultats expérimentaux. Le rapport du nombre d'ions Xe^{2+} au nombre d'ions Xe^{+} varie avec la durée τ de l'impulsion laser comme $\tau^{-3/2}$.

Abstract. — Xe^{2+} ions can easily be formed by multiphoton absorption in Xe atoms at 0.53 μm. At low laser intensities, a laser-Xe atom interaction takes place which generates Xe^{2+} ions through a 15-photon absorption from Xe atoms. At higher intensities, a laser-Xe^{+} ion interaction takes place, generating Xe^{2+} ions through a 10-photon absorption from the Xe^{+} ion in its ground state. The former process is very sensitive to the laser pulse duration in the 5-200 ps range used here. As an example, the number of Xe^{2+} ions is increased by a factor of 30 when the pulse duration is decreased from 30 to 5 ps. The laser intensity at which this occurs is approximately 10^{12} W.cm^{-2}. A kinetic model is developed which is based on the rate equations describing the evolution of populations of Xe atoms, Xe^{+} and Xe^{2+} ions. The result is that the ratio of the number of Xe^{2+} to Xe^{+} ions varies with the pulse duration τ as $\tau^{-3/2}$.

1. Introduction.

The absorption of a very large number of photons by a rare gas atom can induce the detachment of several electrons. Up to quadruply charged ions can be formed with Xe and Kr in the 10^{13} W.cm^{-2} laser intensity range at 1.06 μm [1, 2] and in the 10^{12} W.cm^{-2} intensity range at 0.53 μm [3]. Recently, the mechanism of the formation of Xe^{2+} ions at 0.53 μm has been elucidated [3]. At lower intensities, two processes compete to cause the depletion of atoms; a one-electron removal through a 6-photon absorption, and a two-electron removal through a 15-photon absorption. In a higher intensity range, after depletion of the neutral atoms in the interaction volume, Xe^{2+} ions are formed *via* a 10-photon absorption which results in the removal of one-electron from the Xe^{+} ion. The number of photons involved in these processes is schematically shown in figure 1. Such measurements can give very valuable new information on the comparative multiphoton absorption rates, in the atomic spectrum to generate singly charged ions, and in the ionic spectrum and the continuum to generate doubly charged ions. Such data are still mostly unknown.

The purpose of the present paper is to investigate laser pulse length effects in the creation of Xe^{2+} ions by multiphoton absorption at 0.53 μm. This example has been selected because the two processes which can produce Xe^{2+} ions, i.e. a direct multiphoton absorption from the ground state of the atom, and a stepwise process *via* the Xe^{+} ion in its ground state, are much more clearly distinguished at 0.53 μm than at 1.06 μm [3]. A mode-locked Nd-Glass laser has been especially built to vary the duration of the single pulse in the 10^{-12}-10^{-10} s time scale.

As far as can be found in spectroscopic tables some

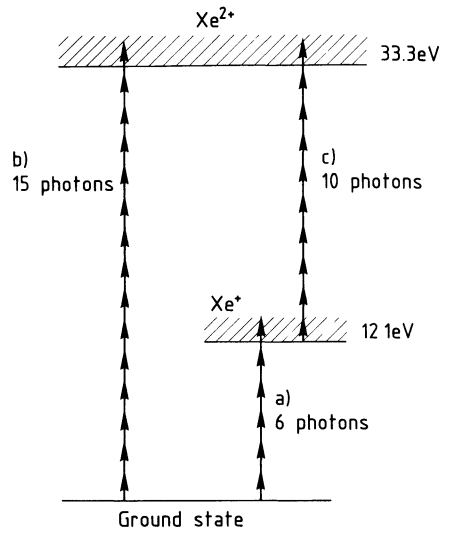

Fig. 1. — Schematic representation of : *a*) the one-electron removal of the Xe atom through a 6-photon absorption; *b*) the two-electron removal of the Xe atom through a 15-photon absorption, and *c*) the one-electron removal of the Xe^{+} ion through a 10-photon absorption.

atomic and ionic states lie in the vicinity, e.g. less than 200 cm^{-1} of a multiple of the laser frequency which is 18,827 $\pm$ 20 cm^{-1}. Unfortunately, no experimental or theoretical data is known in the literature about A. C. Stark shifts of rare gases under a 10^{12} $W.cm^{-2}$ laser field. The only means to study a resonance effect would be to use a tunable wavelength laser ; this will be done in the future.

2. Experimental method.

2.1 THE LASER SYSTEM. — The laser used in the present experiment originates from that described in a previous paper [4]. It is a mode-locked Nd-glass oscillator using Kodak 9740 saturable dye. Figure 2 shows the main elements of the oscillator. In order to generate reproducible pulses of about 5 ps duration, the laser bandwidth is narrowed by putting a highly dispersive prism in the cavity. It is set at the angle of minimum deviation, with the entry and exit of the laser beam at the Brewster angle. This prism reduces the spectrum to a width of 0.4 nm which corresponds to bandwidth-limited pulses of 5 ps at 1.062 μm. Inserting supplementary dispersive elements into the cavity allows us to narrow the laser bandwidth and consequently to lengthen the pulse duration. Using either the prism alone or the prism with one or two Fabry-Perot etalons allows us to vary the pulse duration between 5 ps and 200 ps at 1.062 μm. Outside the cavity, a single pulse is isolated from the mode-locked train by the well-known method of a Pockels switch. The single pulse is selected from the rising edge of the train, where pulses are usually bandwidth-limited. This single pulse is amplified by two Nd-glass preamplifiers and passes through a spatial filter before entering a three-stage Nd-glass amplifier. Then a telescope is used to collimate the beam before it enters a type II KDP doubling crystal. Energies of up to 0.2 J are generated at 0.531 μm with a conversion efficiency of 40 %.

The laser intensity is varied by using the following method. A half-wave plate is placed between the two preamplifiers, and a polarizer is added at the end of the amplifiers chain. The laser intensity is then varied by rotating the half-wave plate. This procedure has the advantage of not modifying the laser beam characteristics, so that the best focus point and the effective focal section remain unchanged. In addition, the polarizer removes any possible birefrigence induced by amplifiers, and gives a well defined linear polarization.

2.2 LASER TEMPORAL AND SPECTRAL DISTRIBUTION. — Two different methods have been used for the measurement of the laser pulse duration in the 5-200 ps range. Pulse durations longer than about 20 ps can be measured accurately with our 5 ps resolution streak camera as described in detail elsewhere [5, 6]. An improvement has been made, the microphotometric analysis of the output of the streak camera being done by using a graphics oriented microcomputer named « Pericolor » [7], coupled with a video acquisition system. This allows the instantaneous determination of the pulse duration at each laser shot. A typical display is represented in figure 3 for

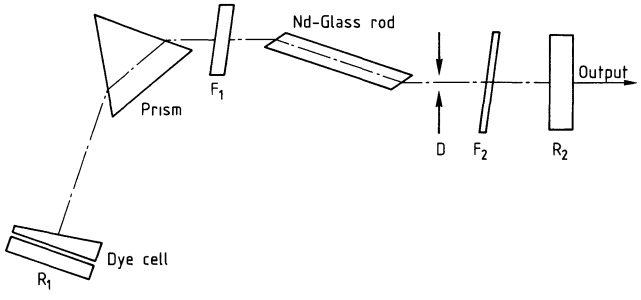

Fig. 2. — Schematic diagram of the mode-locked Nd-glass oscillator. F_1 and F_2 are Fabry-Perot etalons; D is a 1.5 mm pinhole; R_1 total reflection mirror; R_2 65 % reflection output mirror.

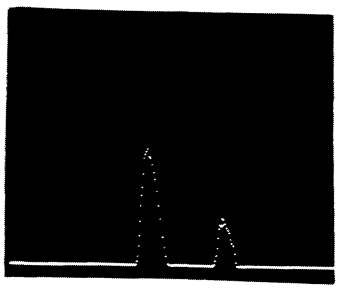

Fig. 3. — Trace of a streak photograph. Temporal scale is given by the pulse separation (200 ps). The top of the smaller pulse determines the level for measuring the FWHM of the main pulse.

a pulse duration of 50 ± 5 ps. The laser pulse has been directed along two paths in order to obtain a time calibration from the length difference between the two. Moreover, one beam has been attenuated by a factor of two, thus directly giving a half-maximum width calibration which does not depend upon the linearity of the total system. A main result is that the duration of the laser pulse obtained at 0.53 μm by second harmonic generation has not been found to vary significantly from the duration of the infrared pulse issued from the laser.

Before entering the streak camera, a fraction of the laser beam is directed onto the entrance slit of a diffraction grating spectrograph. This spectrograph has a dispersion of 1.6 Å/mm at 1.06 μm and is connected to a video recording device which allows one to record the laser spectrum at each shot [5, 6]. The spectral width of an infrared pulse is measured to be 0.45 ± 0.05 Å when the pulse duration is 50 ± 5 ps. The pulse is bandwidth-limited with the corresponding time frequency product being $\Delta t.\Delta \nu = 0.65$.

For pulses shorter than about 20 ps, we have used an indirect procedure which is based on the afore-mentioned time frequency product calibrated with our streak camera. A reflexion from a rod amplifier is directed to the spectrograph and the spectrum of the infrared pulse is recorded at each shot. The pulse duration is deduced from the time frequency product $\Delta t.\Delta \nu = 0.65$. This method, through indirect, is perfectly adequate and convenient for the measurement of pulse durations used here, especially for very short pulse durations as 5 ps.

2.3 GENERAL EXPERIMENTAL SET UP. — The arrangement used in the present study is similar to that adopted for previous experiments [1-3]. The laser pulse is focused into a vacuum chamber (4×10^{-9} torr) by a 75 mm focal length $f/3$ lens corrected for spherical aberration. The ions resulting from the laser interaction with the atoms in the focal volume are extracted with a transverse electric field of 2.5 $kV.cm^{-1}$, separated by a time-of-flight spectrometer and then detected by an electron multiplier. An innovation in the set up consists in a 1 mm circular aperture at the entrance of the time-of-flight spectrometer and differential pumping which keeps the pressure down to 4×10^{-6} torr in the spectrometer when the pressure near the focal region is about 1.7×10^{-4} torr. With this arrangement no complication from possible collisions in the time-of-flight spectrometer are observed. The time-of-flight system is 20 cm long and its resolution is quite adequate to resolve the ion signals corresponding to different charges. From 1 to 10^5 ions are generally formed.

3. Experimental results.

This experiment consists in a measurement of the number of xenon ions formed as a function of the laser intensity for different pulse durations between 5 and 200 ps. Up to Xe^{4+} ions are formed, as was shown by previous results obtained at 0.53 μm with a 50 ps pulse duration [3]. However, in the present work, we are only interested in Xe^{2+} ions in order to investigate laser pulse duration effects on the probability of formation of Xe^{2+} ions. Figures 4, 5 and 6 show typical results obtained with three different pulse durations, respectively 5, 30 and 200 ps. As the sensitivity of an electron multiplier to doubly charged ions is enhanced by a factor of approximately two relative to detection of singly charged ions, experimental points obtained for Xe^{2+} ions have been corrected accordingly. This correction factor comes from the fact that a doubly charged ion gains twice as much energy as a singly charged ion accelerated through the same electric field. The secondary emission coefficient of the first dynode of the electron multiplier is consequently altered. Accurate correction factors for multiply charged rare gas ions are found in the literature [8].

The laser intensity has not been measured in absolute value in the present experiments. However, a comparison can be done with previous results obtained in the same conditions with a fixed 50 ps

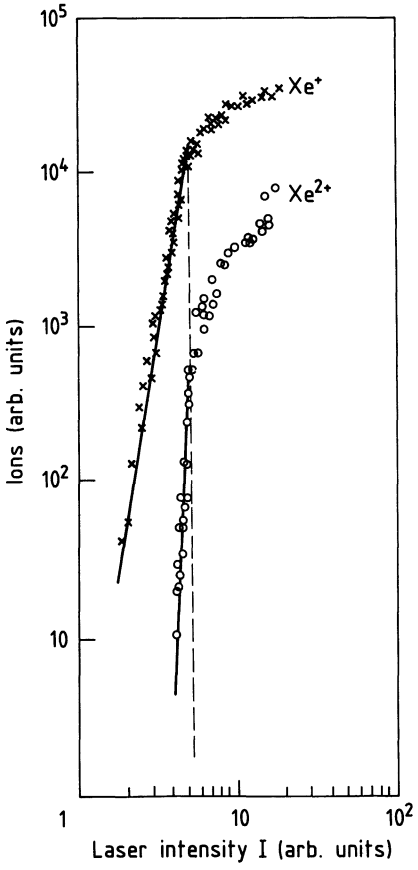

Fig. 4. — Laser pulse duration 5 ps. A log-log plot of the variations in the number of Xe^+ and Xe^{2+} ions formed as a function of laser intensity I. The vertical dashed line indicates the saturation intensity I_S which induces a marked change in the intensity dependence of Xe^+ and Xe^{2+} ions.

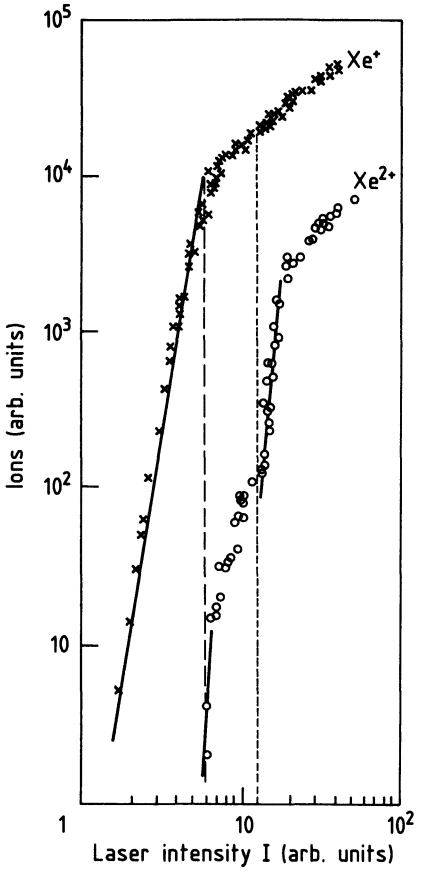

Fig. 5. — Laser pulse duration 30 ps. A log-log plot of the variation in the number of Xe^+ and Xe^{2+} ions formed as a function of the laser intensity I. The vertical dashed line indicates the saturation intensity I_S. The vertical dotted line defines a laser-Xe atom interaction on the left-hand side, and a laser-Xe^+ ion interaction on the right-hand side.

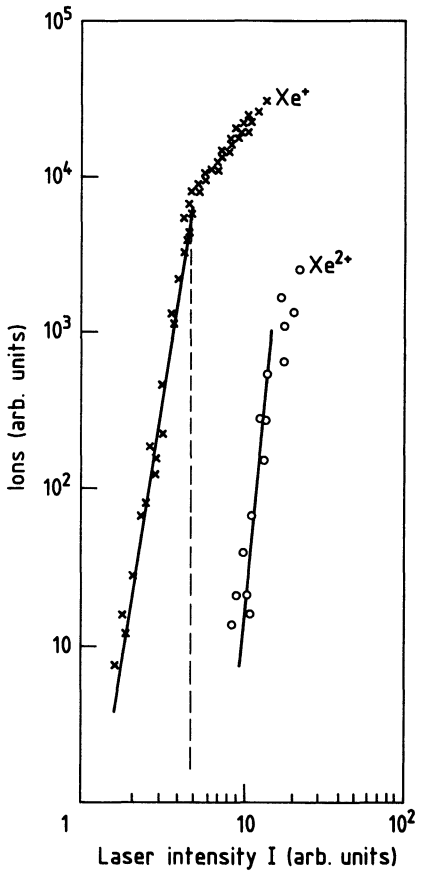

Fig. 6. — Laser pulse duration 200 ps. A log-log plot of the variation in the number of Xe^+ and Xe^{2+} ions formed as a function of the laser intensity I.

laser pulse [3]. The saturation intensity I_S was 8×10^{11} W.cm^{-2}. It should be recalled that the saturation intensity I_S is a convenient intensity reference from which a marked change takes place in the variation of the number of Xe^+ ions as a function of the laser intensity, as shown in figures 4, 5 and 6. This saturation is a typical effect which occurs in multiphoton ionization when all the atoms contained in the interaction volume are ionized [9]. The intensity dependence beyond the I_S value arises from Xe^+ ions formed in the expanding interaction volume. The main difficulty in the present experiment lies in the fact that changing the laser pulse duration results in a small shift of the Xe^+ ion curves along the laser intensity axis, because the probability of creating Xe^+ ions is proportional to $I^N \tau$, in which I is the laser intensity, τ the pulse duration and N the non-linear order : $N = 6$. For example, if we consider a saturation intensity $I_S = 8 \times 10^{11}$ W.cm^{-2} for $\tau = 50$ ps, it would become $I_S = 8.7 \times 10^{11}$ W.cm^{-2} for $\tau = 30$ ps, and $I_S = 1.2 \times 10^{12}$ W.cm^{-2} for $\tau = 5$ ps. Such a change in I_S is less than the uncertainty within which the focused laser intensity can be measured in absolute value in the 10^{12} W.cm^{-2} range. This is the reason why the laser intensity is not expressed in absolute value in figures 4, 5 and 6.

3.1 5 ps PULSE RESULTS. — Figure 4 is a log-log plot of the variation in the number of Xe^+ and Xe^{2+} ions formed as a function of the laser intensity I. For Xe^+ ions, the variation of the number (N^+) of Xe^+ ions as a function of the laser intensity I, has a slope on a log-log plot of $\frac{\partial \text{ Log } N^+}{\partial \text{ Log } I} = 6.0 \pm 0.4$. This slope is the same as the minimum number of photons needed to attain the ionization potential, defined as the next integer above the first ionization energy of the Xe atom (12.1 eV) divided by the laser photon energy (2.335 eV). It is a typical result for a non resonant six-photon ionization process.

As far as Xe^{2+} ions are concerned, the slope $\frac{\partial \text{ Log } N^{2+}}{\partial \text{ Log } I} = 14.5 \pm 1$ is seen before the saturation intensity I_S is reached. The value of the slope is measured accurately for the first time and is in good agreement with the number 15 defined as the next integer above the ratio $E_2/h\nu$, where E_2 is the second ionization energy of the xenon atom (33.3 eV) measured from the ground state of the Xe atom. In addi-

tion, the saturation on the Xe^{2+} ion curve occurs at the same laser intensity I_S as for the Xe^+ ion curve. These two experimental facts : the Xe^{2+} ion curve slope and the same saturation intensity I_S for Xe^+ and Xe^{2+} ion curves, support the assumption of a direct process for the generation of Xe^{2+} ions through a 15-photon absorption from the ground state of the Xe atom. Furthermore, the Xe^{2+} ion yield rises again at the highest laser intensity used, as shown in figure 4. This marks the beginning of another process of formation of Xe^{2+} ions as shown much more clearly in figures 5 and 6 for results obtained with longer laser pulses. Finally, at saturation intensity I_S, the ratio of the number of Xe^{2+} to Xe^+ ions is 3×10^{-2}. This ratio will be used later on for suitable comparison with results obtained using longer pulse durations.

It should be emphasized that single ionization has an order of non-linearity equal to 6, at the same laser intensity where double ionization has 15. This would mean that the intensity dependence of Xe^+ ions is not significantly changed by the absorption of additional photons in the Xe^+ continuum. This point was also checked in a previous paper [2]. As in preceding papers [1-3] on multiply charged ions induced by multiphoton absorption, it should also be emphasized here that the 15-photon absorption which excites two electrons and results in the formation of Xe^{2+} ions has a rate only about 30 times less than that of the 6-photon absorption which excites one electron and gives Xe^+ ions at the saturation intensity 10^{12} W.cm^{-2}. Such a result appears to indicate that absorption of photons in the two-electron spectrum is significantly larger than in the discrete spectrum. This key point in the formation of multiply charged ions through multiphoton absorption is not yet clearly understood. The basic explanation could lie in electron correlation effects.

3.2 30 ps PULSE RESULTS. — Figure 5 shows the results obtained with a 30 ps laser pulse. Here, the probability of creating Xe^{2+} ions through a direct 15-photon absorption from the ground state of Xe atoms has dramatically decreased. At saturation intensity $I_S = 8.7 \times 10^{11}$ W.cm^{-2} the ratio of the number of Xe^{2+} to Xe^+ ions is only 10^{-3}, i.e. 30 times less than in figure 4 with a 5 ps pulse. The Xe^{2+} ion yield curve saturates for intensity beyond I_S, like the Xe^+ ion yield curve, due to depletion of neutral atoms in the interaction volume. When the laser intensity is still further increased, a sudden increase in the Xe^{2+} ion yield curve occurs. The slope of this part of the Xe^{2+} ion yield curve is 9 ± 1. It comes from a stepwise process *via* the Xe^+ ion in its ground state (Fig. 1). As was shown in a previous paper [3], the intensity dependence of this stepwise process is only governed by the 10-photon absorption by Xe^+ ion when the 6-photon process is saturated as it is here. This explains why the slope of this part of the Xe^{2+} ion yield curve is roughly ten.

In short, the Xe^{2+} ion yield curve in figure 5 can be divided into two parts by the vertical dotted line. On the left-hand side, a laser-atom interaction takes place which generates Xe^{2+} ions through a direct 15-photon absorption from Xe atoms. This process saturates for laser intensity beyond I_S when neutral atoms in the interaction volume are depleted. On the right-hand side of the vertical dotted line, a laser-Xe^+ ion interaction takes place that generates Xe^{2+} ions through a 10-photon absorption from the Xe^+ ion in its ground state. This process also saturates at very high intensity.

3.3 200 ps PULSE RESULTS. — Figure 6 shows typical results obtained with a 200 ps laser pulse. In these conditions, the probability of creating Xe^{2+} ions through a direct 15-photon absorption from the ground state of Xe atoms has decreased so much that no Xe^{2+} ions are observed in a range of intensity $I < I_S$. It is only at higher intensity that the stepwise process characterized by the I^{10} law gives rise to Xe^{2+} ions.

As a summary, the « atomic » process which generates Xe^{2+} ions through the direct 15-photon absorption from Xe atoms is very sensitive to the laser pulse duration in the 5-200 ps range used here. This effect will be discussed in the following section. On the contrary, the « ionic » process which generates Xe^{2+} ions through the 10-photon absorption from Xe^+ ions is practically insensitive to the laser pulse duration in the 5-200 ps range. This last result could be tentatively explained in terms of a simple argument similar to that used at the beginning of the present section. It is shown that changing the laser pulse duration results in shifting slightly the Xe^+ ion curve along the laser intensity axis because the single ionization probability is proportional to the product $I^6 \tau$. Here, in the same way changing the laser pulse duration results only in shifting slightly the Xe^{2+} ion curve along the laser intensity axis because the probability of creating Xe^{2+} ions from Xe^+ ions is proportional to $I^{10} \tau$. This shift represents a factor of 1.4 on the laser intensity from 5 to 200 ps and cannot be experimentally detected.

4. Kinetic model.

The kinetic model used here has been described in detail and successfully applied in previous papers [2, 3]. Briefly, the aim of this model is the description of the relative populations of neutral atoms, singly charged ions and doubly charged ions submitted to the three following processes during the interaction with the laser field :

a) one-electron removal from the neutral atom;

b) two-electron removal from the neutral atom;

c) one-electron removal from the singly charged ion.

These processes are schematically shown on figure 7. Volume effects are then dealt with by carefully introducing a spatial laser intensity distribution and integrating the relative populations obtained at the end of the interaction in each spatial point. The method has been greatly improved as compared to the one used before [2, 3] and pulse duration effects have been investigated.

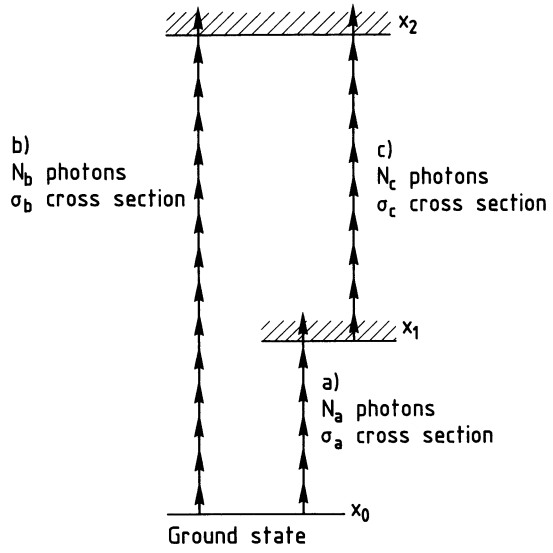

Fig. 7. — Schematic representation of the three processes taken into account in the calculation : *a*) one-electron removal from the neutral atom population x_0 through the absorption of N_a photons, with a cross section σ_a, *b*) two-electron removal from the neutral atom population x_0 through the absorption of N_b photons, with a cross section σ_b, and *c*) one-electron removal from the singly charged ion population x_1 through the absorption of N_c photons, with a cross section σ_c.

The evolution of the relative populations of neutral, singly ionized and doubly ionized atoms, respectively x_0, x_1, x_2, is described by the following system of differential equations :

$$\frac{dx_0}{dt} = -\sigma_a I^{N_a} x_0 - \sigma_b I^{N_b} x_0 \qquad (1a)$$

$$\frac{dx_1}{dt} = \sigma_a I^{N_a} x_0 - \sigma_c I^{N_c} x_1 \qquad (1b)$$

$$\frac{dx_2}{dt} = \sigma_c I^{N_c} x_1 + \sigma_b I^{N_b} x_0 . \qquad (1c)$$

Ionization rates are assumed to be given by lowest order perturbation theory. N_a, N_b, N_c are the non linear orders and σ_a, σ_b, σ_c the generalized cross-sections for the three processes described above (Fig. 7). The laser intensity I depends upon both time and volume and has been chosen to best represent the experimental laser intensity distribution, which has been shown previously to be [2, 3] :

$$I(v, t) = I_M F(v) G(t) \qquad (2)$$

where I_M is the maximum intensity, $F(v)$ and $G(t)$ are the normalized spatial and temporal intensity distributions :

$$F(v) = \exp(-R^2/(1 + Z^2))/(1 + Z^2) \qquad (3)$$

$$G(t) = \cosh^{-1}(2.63\, t/\tau) \qquad (4)$$

in which R and Z are dimensionless cylindrical coordinates and τ the pulse duration. The system (1) of differential equations is solved partly analytically, partly numerically. Then integrating over the volume, the populations of singly and doubly charged ions produced during the interaction are obtained for each given maximum intensity I_M. Cross-sections σ_a, σ_b, σ_c were determined previously [3] by fitting the experimental curves obtained with a 50 ps Nd YAG laser at 0.53 μm. They are summarized in table I. The uncertainties mainly come from the error on the absolute value of the laser intensity which is about 40 % and greatly exceeds the one due to the fit itself between calculated curves and experimental ones. It should be emphasized that those measurements were the first determinations of multiphoton double ionization cross-sections and multiphoton ionization cross-sections for singly charged ions.

Table I. — *The generalized* N*-photon ionization cross sections* σ_a, σ_b *and* σ_c *corresponding respectively to the one-electron removal of the* Xe *atom through a* 6*-photon absorption, the two-electron removal of the* Xe *atom through a* 15*-photon absorption, and the one-electron removal of the* Xe^+ *ion through a* 10*-photon absorption. They are expressed in* $W^{-N}.cm^{2N}.s^{-1}$ *and in* $cm^{2N}.s^{-1}$.

	σ_a	σ_b	σ_c
$W^{-N}.cm^{2N}.s^{-1}$	$10^{-61\pm1}$	$10^{-172\pm3}$	$10^{-115\pm2}$
$cm^{2N}.s^{N-1}$	$10^{-171\pm1}$	$10^{-448\pm3}$	$10^{-299\pm2}$

In order to draw out the duration effects, let us introduce the dimensionless variable $u = t/\tau$ and the normalized intensity distribution $D(u)$, which is the product of the spatial distribution and the temporal distribution, where t/τ has been replaced by u. The system (1) of differential equations can be written :

$$\frac{dx_0}{du} = -\sigma_a I_M^{N_a} \tau D(u)^{N_a} x_0(u) - \sigma_b I_M^{N_b} \tau D(u)^{N_b} x_0(u) \qquad (5a)$$

$$\frac{dx_1}{du} = \sigma_a I_M^{N_a} \tau D(u)^{N_a} x_0(u) - \sigma_c I_M^{N_c} \tau D(u)^{N_c} x_1(u) \qquad (5b)$$

$$\frac{dx_2}{du} = \sigma_c I_M^{N_c} \tau D(u)^{N_c} x_1(u) + \sigma_b I_M^{N_b} \tau D(u)^{N_b} x_0(u) . \qquad (5c)$$

The pulse duration influence upon these kinetic equations appears in the evolution rates of the populations. As was shown in figures 4, 5, 6 the shortening of the pulse duration induces a dramatic increase of the number of Xe^{2+} ions formed by a direct 15-photon ionization process from the ground state of the atoms. This experimental result is reproduced by the sets of curves obtained from calculations which have been performed with different pulse durations from 5 to 200 ps. Moreover, the agreement between experimental data and calculated curves remains good as is shown for example at 30 and 200 ps on figures 8 and 9. The calculated Xe^{2+} curve deviates noticeably from the experimental points in figure 8 at very high intensity. An explanation could be that the 1 mm aperture at the entrance of the time of flight spectrometer is not accounted for in the numerical calculations while the length of the focal volume that contributes at very high intensity is a little longer than 1 mm. A second possible explanation is that Xe^{3+} ions are not taken into account in the present numerical calculations.

A more precise comparison between experimental and calculated data can be made by introducing :

$$R = \frac{x_2/x_1 \ (5 \text{ ps})}{x_2/x_1 \ (30 \text{ ps})} \tag{6}$$

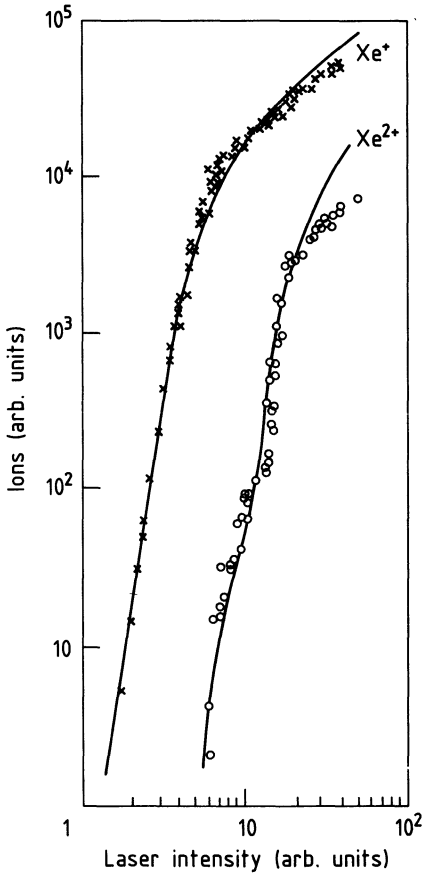

Fig. 8. — Curves (in solid line) calculated from the kinetic model presented in § 4, with experimental data obtained at 30 ps.

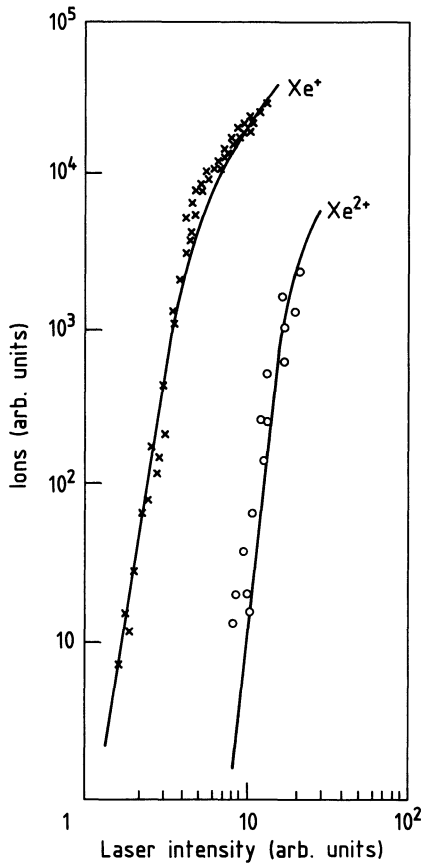

Fig. 9. — Calculated curves in solid line and experimental data obtained at 200 ps.

x_2/x_1 being the ratio of doubly to singly charged ions obtained at 5 and 30 ps respectively at the saturation intensity I_S. The ratio R_{exp} obtained from experimental results is equal to 30, with a precision not better than 50 %, due to the scatter in the experimental points.

The theoretical saturation intensity I_S^{th} is defined by :

$$\sigma_a (I_S^{th})^{N_a} \tau_{N_a} = 1 \tag{7}$$

in which

$$\tau_{N_a} = \int_{-\infty}^{+\infty} G^{N_a}(t) \, dt \tag{8}$$

I_S^{th} differs very slightly from the experimental saturation intensities given in section 3. I_S^{th} is equal to 8×10^{11} W.cm^{-2} at 30 ps, 1.1×10^{12} W.cm^{-2} at 5 ps. The ratio obtained is $R_{th} = 18.8$, in reasonable agreement with the experimental value. The kinetic model is thus well fitted to describe the relative populations of the different ion species when the pulse duration is varied.

Finally, a graphical representation of pulse duration effects is shown on figure 10. The abcissa represents the product $I_M \tau^{1/N_a}$. The single ionization probability being proportional to $I_M^{N_a} \tau$, the Xe^+ ion curves for different pulse durations are superimposed and represented by a dashed line. Three Xe^{2+} ion curves obtained at 5, 30 and 200 ps are drawn as solid lines.

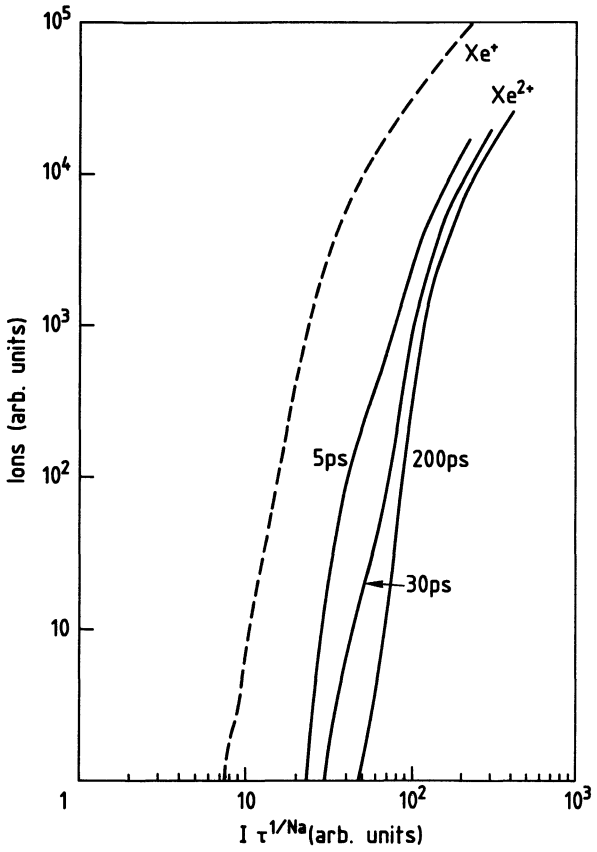

Fig. 10. — The number of Xe^{2+} and Xe^{+} ions deduced from the kinetic model has been plotted as a function of the variable $\tau^{1/N_a} I$. The number of Xe^{+} ions, which does not vary when τ is decreased, has been drawn in dashed lines. Three Xe^{2+} ions curves are obtained at 5, 30, 200 ps.

This figure clearly describes the effect of pulse duration, i.e. the decrease of the probability of creating doubly charged ions when the pulse duration is increased.

5. Discussion.

In order to make pulse duration effects clearer, let us consider simpler assumptions which will allow us to have a qualitative analytical representation of these effects. The process (c), creation of doubly charged ions from singly charged ions, is not taken into account. Volume effects are neglected and the temporal distribution is assumed to be a square pulse of width equal to τ.

The numbers x_1, x_2 of ions formed at the end of the pulse and their ratio are easily derived from system (1) :

$$x_1 = \frac{\sigma_a I^{N_a}}{\sigma_b I^{N_b} + \sigma_a I^{N_a}} \times \times (1 - \exp(-\sigma_a I^{N_a} \tau - \sigma_b I^{N_b} \tau)) \quad (9a)$$

$$x_2 = \frac{\sigma_b I^{N_b}}{\sigma_b I^{N_b} + \sigma_a I^{N_a}} \times \times (1 - \exp(-\sigma_a I^{N_a} \tau - \sigma_b I^{N_b} \tau)) \quad (9b)$$

$$\frac{x_2}{x_1} = \frac{\sigma_b I^{N_b}}{\sigma_a I^{N_a}}. \quad (10)$$

This ratio does not seem to depend on the pulse duration. However, as the relative efficiencies of single and double ionization processes are compared for different pulse durations, this ratio has to be evaluated for a constant single ionization probability; i.e. for $I_M^{N_a} \tau$ constant, so that it actually appears as :

$$\frac{x_2}{x_1} = B\tau^{\frac{N_a - N_b}{N_a}} \quad (11)$$

in which B is a constant independent of the intensity.

For xenon at 0.53 μm, the ratio x_2/x_1 varies as $\tau^{-3/2}$ and hence rapidly increases as τ is shortened. As a result, the laser pulse duration appears to be a very flexible parameter with which to change the proportion of Xe^{2+} to Xe^{+} ions formed respectively through 15 and 6-photon absorption from xenon atoms.

Laser pulse duration effects investigated here through the relative ratio of Xe^{2+} to Xe^{+} ions have a much more general implication in all non linear processes. When two different non linear processes competitively deplete a population of atoms, the highest order process is expected to increase more than the lowest order when the interaction time is shortened. The formation of Xe^{2+} ions just below the saturation takes place simultaneously with the absorption of several additional photons above the first ionization threshold in the one-electron removal of Xe atoms. This latter process has been investigated previously by measuring the energy spectrum of the photoelectrons [10, 11]. This spectrum consists of a series of peaks spaced by an amount equal to the photon energy. The absorption of three and even four additional photons above the first ionization threshold has been observed at 0.53 μm. Laser pulse length effects described in the present paper could play a similar rôle in the relative amplitude of the different peaks in the energy spectrum of electrons. Such aspects have already been considered in two theoretical papers [12, 13].

6. Conclusion.

A mode-locked Nd-glass laser with variable pulse duration (5 to 200 ps) has been used to investigate pulse length effects on the formation of Xe^{2+} ions produced by multiphoton absorption at 0.53 μm. Xe^{2+} ions can be formed through two different processes. In a lower laser intensity range, a laser-Xe atom interaction takes place which generates Xe^{2+} ions through a direct 15-photon absorption from Xe atoms, while in a higher intensity range, a laser-Xe^{+} ion interaction takes place which generates Xe^{2+} ions through a 10-photon absorption from the Xe^{+} ion in its ground state. The latter process is not significantly affected by the pulse duration. In contrast, the former process is very sensitive to the pulse duration in the 5-200 ps range used here. As an example, the number of Xe^{2+} ions is increased by a factor 30

when the pulse duration is decreased from 30 ps to 5 ps, at an intensity approximately equal to 10^{12} W.cm^{-2}.

A kinetic model has been developed based on the rate equations describing the evolution of populations of neutrals as well as singly and doubly charged ions. It perfectly describes pulse duration effects observed here. By neglecting the one-electron removal from singly charged ion, a simple qualitative analytical expression can be derived. It exhibits a pulse duration τ dependence of $\tau^{-3/2}$ for the ratio of the population of doubly to singly charged ions at the saturation intensity, in the pulse duration range (5-200 ps) used in the present experiment.

The laser pulse duration appears as a very flexible parameter to change the relative population of doubly to singly charged ions formed through multiphoton absorption. Moreover, laser pulse length effects have a more general implication in every non linear processes. When two different non linear processes competitively deplete the same population, the highest order process is expected to increase more than the lowest order process when the interaction time is shortened.

Furthermore, in an experiment in progress at 1.06 μm, Xe^{2+} ions do not seem to be significantly affected by the pulse duration. This is most likely because the two processes *b*) and *c*) mentioned above which induce Xe^{2+} ions are superimposed at 1.06 μm and not as well separated as at 0.53 μm.

Finally, more information on the basic processes involved in the formation of multiply-charged ions would be available with a tunable-wavelength laser. Experiments of that kind will be performed in the near future.

Acknowledgments.

We are grateful to M. Poirier and Dr. J. Reif for very valuable discussions, to J. Thebault and B. Calvel for help with measurements and to D. Fondant for assistance with experiments.

References

[1] L'HUILLIER, A., LOMPRÉ, L. A., MAINFRAY, G. and MANUS, C., *Phys. Rev. Lett.* **48** (1982) 1814.

[2] L'HUILLIER, A., LOMPRÉ, L. A., MAINFRAY, G. and MANUS, C., *J. Phys. B* **16** (1983) 1363.

[3] L'HUILLIER, A., LOMPRÉ, L. A., MAINFRAY, G. and MANUS, C., *Phys. Rev. A* **27** (1983) 2503.

[4] LOMPRÉ, L. A., MAINFRAY, G., MANUS, C. and THEBAULT, J., *J. Physique* **39** (1978) 610.

[5] LOMPRÉ, L. A., MAINFRAY, G. and THEBAULT, J., *Appl. Phys. Lett.* **26** (1975) 501.

[6] LOMPRÉ, L. A., MAINFRAY, G. and THEBAULT, J., *J. Appl. Phys.* **48** (1977) 1570.

[7] LOMPRÉ, L. A., MAINFRAY, G. and THEBAULT, J., *Revue Phys. Appl.* **17** (1982) 21.

[8] SCHRAM, B., BOERBOOM, A., KLEINE, W. and KISTEMAKER, J., Proceedings of the Seventh Intern. Conf. on Phenomena in Ionised Gases, Belgrade 1965, edited by Perovio B. and Tosic D., Belgrade 1966, vol. 1, p. 170.

[9] CERVENAN, M. and ISENOR, N., *Opt. Commun.* **13** (1975) 175.

[10] AGOSTINI, P., CLEMENT, M., FABRE, F. and PETITE, G., *J. Phys. B* **14** (1981) L-491.

[11] KRUIT, P., KIMMAN, J. and VAN DER WIEL, M., *J. Phys. B* **14** (1981) L-597.

[12] CRANCE, M. and AYMAR, M., *J. Phys. B* **13** (1980) L-421.

[13] GONTIER, Y. and TRAHIN, M., *J. Phys. B* **13** (1980) 4383.